

# Quantum Gravity Effects on the Tachyon Inflation from Thermodynamic Perspective

M. Bitaj<sup>1</sup>, N. Rashidi<sup>2</sup>, K. Nozari<sup>3</sup> and M. Roushan<sup>4</sup>

Department of Theoretical Physics, Faculty of Science, University of Mazandaran,  
P. O. Box 47416-95447, Babolsar, IRAN

## Abstract

By considering the Friedmann equations emerging from the entropy-area law of black hole thermodynamics in the context of the generalized uncertainty principle, we study tachyon inflation in the early universe. The presence of a minimal length modifies the Friedmann equations and hence the slow-roll and perturbation parameters in the tachyon model. These modifications, though small, affect the viability of the tachyon inflation in confrontation with observational data. We compare the numerical results of the model with Planck2018 TT, TE, EE +lowE+lensing+BAO+BK14(18) data and Planck2018 TT, TE,EE +lowE+lensing+BK14(18) +BAO+LIGO & Virgo2016 data at 68% and 95% CL. We show that while the tachyon inflation with power-law, inverse power-law and inverse exponential potentials is not observationally viable in comparison with the  $1\sigma$  and  $2\sigma$  confidence levels of the new joint data, in the presence of the minimal length the model becomes observationally viable.

**PACS:** 98.80.Bp, 98.80.Cq, 98.80.Es

**Key Words:** Tachyon Inflation; Minimal Length; Observational Viability.

---

<sup>1</sup>mozhdeh.bitaj@gmail.com

<sup>2</sup>n.rashidi@umz.ac.ir (Corresponding Author)

<sup>3</sup>knozari@umz.ac.ir

<sup>4</sup>m.roushan@umz.ac.ir

# 1 Introduction

All approaches to quantum gravity proposal predict the existence of a fundamental length scale of the order of the Planck (or fundamental string) length, below of which no distinction/resolution of the spacetime points is possible [1]. In fact, black hole physics [2] together with all phenomenological approaches to QG proposal including String Theory [1, 3, 4, 5], Loop Quantum Gravity [6, 7, 8, 9], Asymptotically Safe Quantum Gravity [10, 11, 12, 13], Noncommutative Geometry [14, 15], Polymer Quantization of spacetime [16] and some Gedanken experiments (thought experiments) proposed to unify Quantum Mechanics and General Relativity [17], all predict the existence of a minimal fundamental measurable length of the order of the Planck length. To incorporate this minimal length in ordinary quantum mechanics, one modifies the Heisenberg Uncertainty Principle to derive the so-called Generalized (Gravitational) Uncertainty Principle (GUP). A GUP setup includes the gravitationally induced position uncertainty associated with the minimal fundamental length scale. On the other hand, the Tachyon inflation has its origin in string theory tachyon condensation and as is known [18], cosmic inflation in these theories occurs at super-Planckian densities; the era of which QG effects are important in essence. If this is the case and as far as we know it is definitely the case, quantum gravity effects encoded in the existence of a minimal length/maximal energy(momentum) have to be incorporated in a Tachyon inflation. In fact, the minimal length/maximal energy as a ultra-violet natural cutoff encoded in the generalized uncertainty principle governs generation of seeds and evolution of the cosmological perturbations. This feature technically is addressed by imposing the existence of the minimal length on the wavelength of acoustic perturbations or equivalently on wave numbers (or equivalently wave's momentum). This is the main motivation for incorporation of the generalized uncertainty principle in this Tachyon inflation scenario.

It is worth noting that some subtleties in transition to relativistic field theory, such as self-adjointness of the position and momentum operators can be addressed via von Neumann theorem through maximally localized states or quasi-position/momentum states in dense domains of these operators in the generalized Bargmann-Fock space (See [19] and Appendix C of [20] for details). About the self-adjointness of the time operator, formally a similar argument is possible in essence, but not in a maximally localized states (or quasi-position/momentum states) in position/momentum spaces, but in a time/energy formal space. Also, doubly special relativity provides a maximal momentum [21, 22] that regularizes the free particle's energy not to be divergent anymore and position (momentum) is actually an operator in the dense domain of  $\{x, x^2\}$  ( $\{p, p^2\}$ ) in maximally localized states or quasi-position (quasi-momentum) representation in Bargmann-Fock space. The details of such arguments can be seen in Refs. [19] and [20].

In the study of the relativistic cosmology, the Friedmann equations are two important equations governing the dynamics of the universe. These equations, which are obtained from the Einstein field equations, have great importance to describe the expansion history of the universe. Interestingly, it has been shown that the Einstein equations can be obtained from the thermodynamic viewpoint by using the Clausius relation between the temperature ( $T$ ), entropy ( $S$ ), and heat ( $Q$ ) [23]. This idea was based on the connection between entropy and horizon area in black hole physics and demanding that through each spacetime point the Clausius relation  $dQ = T dS$  holds for all the local Rindler causal horizons. In this context, the Einstein field equations are claimed to be an equation of state for the considered spacetime (see [23] for more details). On the other hand, Verlinde [24] has shown that the Friedmann equation governing the dynamics of the FRW spacetime can be rewritten in the same form as the entropy formula which governs the thermodynamics of radiation component in the

universe. See also [26, 25, 27, 28] for more literature on this issue. Overall, it seems that there are some relations between thermodynamics and Einstein equations and this is an interesting subject to be studied in more relevant backgrounds. In this regard, the authors of [29] have obtained  $(n + 1)$ -dimensional Friedmann equation for the FRW universe, based on the thermodynamic perspective. Their approach was based on the following relations for the temperature  $T$  and entropy  $S$  of the apparent horizon

$$T = \frac{1}{2\pi\tilde{r}_A}, \quad (1)$$

$$S = \frac{A}{4G}, \quad (2)$$

where  $\tilde{r}_A$  is the apparent horizon radius of the universe,  $G$  is the Newton constant and  $A$  is the apparent horizon area. They have started their work by considering the following  $(n + 1)$ -dimensional FRW metric

$$ds^2 = -dt^2 + a^2(t) \left( \frac{dr^2}{1 - k r^2} + r^2 d\Omega_{n-1}^2 \right), \quad (3)$$

where  $k = 0, \pm 1$  shows the spatial curvature constant and  $d\Omega_{n-1}^2$  is the line element of an  $(n - 1)$ -dimensional unit sphere. By rewriting the line element (3) as

$$ds^2 = h_{ij} dx^i dx^j + \tilde{r}^2 d\Omega_{n-1}^2, \quad (4)$$

where  $h_{ij}$  is a two-dimensional metric as  $(-1, a^2/(1 - kr^2))$ ,  $\tilde{r} = a(t)r$  and  $x^i = (t, r)$ , they have obtained the apparent horizon  $\tilde{r}_A$  in terms of the Hubble parameter  $H$ . Then, by using the first law of thermodynamics and the relation between the apparent horizon temperature and the surface gravity, they obtained the Friedmann equation for an  $(n + 1)$ -dimensional universe as

$$H^2 = \frac{16\pi G}{n(n-1)}\rho - \frac{k}{a^2}, \quad (5)$$

where  $\rho$  is the energy density of the components inside the apparent horizon. See Ref. [29] for more details on obtaining Friedmann equation (5).

Another interesting subject is the connection between the uncertainty principle and Hawking radiation in the black hole physics context [30, 31, 32, 33, 34, 35, 36]. Especially, the idea of the Generalized Uncertainty Principle (GUP), proposed in black hole physics (and also string theory), has attracted a lot of attention. There is a belief that there is a minimal length implied by quantum gravitational considerations, leading to the modified uncertainty principle as [32]

$$\Delta x_i \gtrsim \frac{\hbar}{\Delta p_i} \left[ 1 + \frac{\beta l_{Pl}^2}{\hbar^2} (\Delta p_i)^2 \right], \quad (6)$$

where  $l_{Pl}$  is the Planck length and  $\beta$  is a dimensionless parameter whose value depends on the specific model. In the  $\Delta x_i \gg l_{Pl}$  limit (classical limit), the equation (6) recovers the standard Heisenberg uncertainty relation as  $\Delta x_i \Delta p_i \geq \hbar \delta_{ij}$  or  $\Delta x \Delta p \geq \hbar$  in one space dimension. From now on, we adopt  $\hbar = 1 = c$ . By considering equation (6), and the argument that the uncertainty principle  $\Delta p \geq \frac{1}{\Delta x}$  is equivalent to  $\Delta E \geq \frac{1}{\Delta x}$  [37], one can find a lower bound on the energy of a test particle in the GUP case, assuming  $E \sim \Delta E$ . Since the area of the black hole and correspondingly,

its entropy is related to the energy, the lower bound on energy gives a modified expression for the entropy. This modification, via the first law of thermodynamics, leads to a modified Friedmann equation [38].

One branch of cosmology, where the Friedmann equations play an important role, is primordial cosmological inflation. In the inflation era, the universe has expanded exponentially in a very short time. A lot of interesting works on inflation have been done which some of them predict gaussian distribution for dominant modes of the perturbations while some others predict non-gaussian distribution [39, 40, 41, 42, 43, 44, 45, 46, 47]. Among the various inflation models, the tachyon inflation is the one with interesting results [48, 49, 50, 51]. In the tachyon inflation, the tachyon field (a non-canonical field associated with the D-branes in string theory) drives the inflation phase of the universe. In this model, the universe evolves smoothly from the accelerating phase of the expansion to the non-relativistic fluid-dominated phase. For some interesting works on tachyon inflation see [52, 53, 54]. Every inflation model, in order to be considered viable, should be consistent with observational data. To check the observational viability of an inflation model, we can perform some numerical analysis on the perturbation parameters such as the scalar and tensor spectral indices ( $n_s$ ) and ( $n_T$ ), respectively and also the tensor-to-scalar ratio ( $r$ ). By comparing the results of the numerical analysis with the newest observational data, we can test the viability of the inflation model. To this end, we should adopt some types of potential. In Ref. [55] the authors have shown that the tachyon inflation can be considered as a stringy implementation of the chaotic inflation. In this regard, it seems interesting to consider chaotic potentials. For instance, a tachyon model with  $\phi^2$  and  $\phi^4$  potentials is not consistent with observational data. In Ref. [56], the tachyon inflation with both  $\phi^2$  and  $\phi^4$  potentials has been considered. The authors have compared this model with Planck2013 results [57] and obtained the observational viability of the model. According to their analysis, for  $\phi^2$  potential, the tachyon model has  $n_s = 0.975$  corresponding to  $r = 0.066$ . Also, for  $\phi^4$  potential, the tachyon model has  $n_s = 0.972$  corresponding to  $r = 0.088$ . Although these values were consistent with Planck 2013 data, now they are out of  $1\sigma$  and  $2\sigma$  confidence level of Planck2018 data. In Ref. [54], the authors have considered several potentials including  $\phi^{-2}$ ,  $\phi^{-4}$  and inverse exponential potential. They have obtained some consistency between the tachyon model with Planck2015 [58]. However, with Planck2018 model these cases rule out.

Given that in the early universe, the energy was very high, it seems that the quantum gravitational effects should be important in the physics of that era. In fact, since existence of a minimal measurable length/ maximal measurable energy, is a phenomenological aspect of all existing approaches to QG proposal, it is natural to seek for its effects on a high energy phenomenon such as the cosmological inflation, the phenomenon that stringy effects are inevitable, at least in Tachyon condensation as the main underlying concept of this setup. If stringy effects are important in high energy regime, then investigation of the effect of this high energy ingredient as a UV cutoff is essentially inevitable. Therefore, it is interesting to consider the quantum gravitational effects in the study of the primordial inflation [27, 52, 59]. In this paper, we include the quantum gravitational effects in the early universe by considering the modified Friedmann equations consisting minimal length effects. In this way, the slow-roll parameters in the inflation model are modified and therefore, the main perturbation parameters (scalar and tensor spectral indices) are modified too. These modifications of the perturbation parameters can change the status of the viability of the model in confrontation with recent observational data. To test the viability of the model, we consider both Planck2018 TT, TE, EE+lowE+lensing+BAO+BK14 data and Planck2018 TT, TE, EE +lowE+lensing+BK14+BAO+LIGO and Virgo2016 data [60, 61]. Also, we exam-

ine the observational viability of this modified model in confrontation with Planck2018 TT, TE, EE+lowE+lensing+BAO+BK18 data and Planck2018 TT, TE, EE +lowE+lensing+BK18+BAO +LIGO and Virgo2016 data [62, 63].

With these preliminaries, this paper is organized as follows. In section 2, we review the reconstruction of the Friedmann equations from the first law of thermodynamics with general expression for the entropy. In section 3, by considering the tachyon field in the model, we present the modified Friedmann equations of the tachyon model in the presence of a minimal length. In section 4, tachyon inflation in the presence of the minimal length is formulated. In section 5, we perform a numerical analysis on the model parameter space and compare the results with several data sets. In this manner, we find the viability of our model in some ranges of the deviation parameter. In section 6, we present a summary of our work.

## 2 Modified Friedmann Equations: Reconstruction from the First Law of Thermodynamics

To reconstruct the modified Friedmann equations, we start with the spatially flat (3+1) dimensional FRW background with the following line element

$$ds^2 = h_{ij} dx^i dx^j + \tilde{r}^2 d\Omega_2^2. \quad (7)$$

We can find the dynamic apparent horizon radius with this line element. This horizon, a marginally trapped surface with the vanishing expansion, is a sphere of radius  $\tilde{r}_A$  that satisfies the following equation [64, 65]

$$h^{ij} \partial_i \tilde{r} \partial_j \tilde{r} = 0. \quad (8)$$

Solving this equation gives the following expression for the apparent horizon in the flat FRW universe [29]

$$\tilde{r}_A = a r = \frac{1}{H}, \quad (9)$$

where  $H$  is the Hubble parameter defined as  $H = \frac{\dot{a}}{a}$ . Note that, an over dot shows a cosmic time derivative. Now, we consider a universe filled with perfect fluid with the following energy-momentum tensor

$$T_{\mu\nu} = (\rho + p) u_\mu u_\nu + p g_{\mu\nu}. \quad (10)$$

In this definition, we have shown the 4-velocity of the fluid with  $u_\nu$ . Also, the energy density and pressure of the perfect fluid are represented with  $\rho$  and  $p$ , respectively. Satisfying the conservation law for  $T^{\mu\nu}$  gives the conservation equation as

$$\dot{\rho} + 3H(\rho + p) = 0. \quad (11)$$

Following Refs. [66, 67], the work function or work density in terms of the trace of the energy-momentum tensor is given by

$$W = -\frac{1}{2} T^{ij} g_{ij}. \quad (12)$$

Note that in equation (12),  $T^{ij}$  is the projection of the (3 + 1)-dimensional energy-momentum tensor  $T^{\mu\nu}$  in the normal direction on the 2-sphere [29]. When we consider a flat FRW universe filled with a perfect fluid, equation (12) gives

$$W = \frac{1}{2}(\rho - p). \quad (13)$$

This work function is important in treating the first law of thermodynamics. The first law of thermodynamics is given by

$$dE = T dS + W dV, \quad (14)$$

where the parameter  $E$  is the total energy inside the apparent horizon or the Misner-Sharp energy and it is defined as [38, 65]

$$E = \rho V. \quad (15)$$

In the above definition,  $V$  is the volume of a 3-dimensional sphere with radius  $\tilde{r}_A$ , given by  $V = \frac{4}{3}\pi\tilde{r}_A^3$ . From equation (15) we get

$$dE = \rho dV + V d\rho. \quad (16)$$

Now, by using equations (11), (15), and (16) we find

$$dE = 4\pi\tilde{r}_A^2 \rho d\tilde{r}_A - 4\pi\tilde{r}_A^3 (\rho + p) H dt. \quad (17)$$

On the other hand, the term  $W dV$  in equation (14) is given by

$$W dV = 2\pi\tilde{r}_A^2 (\rho - p) d\tilde{r}_A. \quad (18)$$

Also, we need to rewrite the term  $T dS$  in equation (14) in terms of  $\tilde{r}_A$ . To this end, in Ref. [38] the authors have used the relationship between temperature and surface gravity as

$$T = \frac{\kappa}{2\pi}. \quad (19)$$

The parameter  $\kappa$  is the surface gravity defined as

$$\kappa = \frac{1}{2\sqrt{-h}} \partial_i \left( \sqrt{-h} h^{ij} \partial_j \tilde{r}_A \right). \quad (20)$$

By considering the metric (7), the surface gravity takes the following form

$$\kappa = -\frac{1}{\tilde{r}_A} \left( 1 - \frac{\dot{\tilde{r}}_A}{2H\tilde{r}_A} \right). \quad (21)$$

On the other hand, as it has been considered in Ref. [38], the general expression for the entropy in terms of area ( $A$ ) is given by

$$S = \frac{f(A)}{4G}. \quad (22)$$

Therefore, from equations (19), (21), and (22) we find

$$T dS = -\frac{1}{2\pi\tilde{r}_A} \left(1 - \frac{\dot{\tilde{r}}_A}{2H\tilde{r}_A}\right) d\left(\frac{f(A)}{4G}\right) = -\frac{1}{2\pi\tilde{r}_A} \left(1 - \frac{\dot{\tilde{r}}_A}{2H\tilde{r}_A}\right) \left(\frac{df(A)}{dA}\right) \left(\frac{8\pi\tilde{r}_A}{4G} d\tilde{r}_A\right). \quad (23)$$

From equation (9), we have  $\dot{\tilde{r}}_A = -\tilde{r}_A^2 \dot{H}$  and  $d\tilde{r}_A = -\tilde{r}_A^2 \dot{H} dt$ . By using these equations and also equations (14), (17), (18) and (23) we find the following expression for the second Friedmann equation

$$\dot{H} \frac{df(A)}{dA} = -4\pi G(\rho + p). \quad (24)$$

From equation (11) and integrating equation (24) we get

$$\rho = -\frac{3}{2G} \int \frac{f'(A)}{A^2} dA, \quad (25)$$

where  $f'(A) = \frac{df(A)}{dA}$ . In the case with  $f(A) = A$ , equations (24) and (25) give the standard Friedmann equations as

$$\dot{H} = -4\pi G(\rho + p), \quad (26)$$

$$H^2 = \frac{8\pi G}{3}\rho. \quad (27)$$

Given that the presence of the minimal length shows itself in the entropy-area relation, and then the entropy-area relation is used to obtain the modified Friedmann equations, in the next section we derive the modified Friedmann equation of the tachyon field in the presence of the minimal length. As has been shown in Ref. [38], this modification is obtained by considering a GUP.

### 3 The Friedmann Equations of the Tachyon Field in the Presence of the Minimal Length

As we have mentioned in the Introduction, the presence of the minimal length modifies the uncertainty principle as equation (6). This equation gives the minimal measurable length scale as  $\Delta x_{min} = 2\sqrt{\beta} l_{Pl}$  and the following expression for  $\Delta p$  [38]

$$\Delta p \gtrsim \frac{1}{2\beta l_{Pl}^2} \left( \Delta x - \sqrt{(\Delta x)^2 - 4\beta l_{Pl}^2} \right). \quad (28)$$

Also, the change in the area of a black hole that absorbs or emits a quantum particle is given by  $\Delta A \geq 8\pi l_{Pl}^2 E R$ , where  $R$  is the particle's size and  $E$  is its energy [68]. By considering the existence of a finite bound, implied by the particle, we have  $\Delta A_{min} \geq 8\pi l_{Pl}^2 E \Delta x$ . Since the uncertainty principle  $\Delta p \geq \frac{1}{\Delta x}$  can be rewritten as  $E \geq \frac{1}{\Delta x}$  [30, 69], from equation (28) we obtain

$$\Delta A_{min} \gtrsim \frac{8\pi \Delta x}{2\beta} \left( \Delta x - \sqrt{(\Delta x)^2 - 4\beta l_{Pl}^2} \right). \quad (29)$$

Now, by assuming  $\Delta x^2 = \frac{A}{\pi}$ , the change in the area is given by [38]

$$\Delta A_{min} \simeq \chi \frac{8A}{2\beta} \left( 1 - \sqrt{1 - \frac{4\beta l_{Pl}^2 \pi}{A}} \right). \quad (30)$$

By using the Bekenstein-Hawking entropy formula, the parameter  $\chi$  can be determined. Now we explore the relationship between entropy and area. Given that the minimal increase of entropy is a bit of information as  $\Delta S_{min} = b = \ln(2)$  [70], and since from the Bekenstein-Hawking entropy formula we have  $\frac{b}{\chi} = 2\pi$  [30], we get

$$\frac{dS}{dA} = \frac{\Delta S_{min}}{\Delta A_{min}} = \frac{\pi}{\frac{2A}{\beta} \left( 1 - \sqrt{1 - \frac{4\beta l_{Pl}^2 \pi}{A}} \right)}. \quad (31)$$

From equation (22), we find  $f'(A) = 4G \frac{dS}{dA}$ . Therefore, by using equation (31) we can rewrite Friedmann equations (24) and (25) as follows

$$\dot{H} \left( \frac{\beta l_{Pl}^2}{2} \right) \left( \frac{H^2}{1 - \sqrt{1 - \beta l_{Pl}^2 H^2}} \right) = -4\pi G (\rho + p), \quad (32)$$

$$\frac{H^2}{2} + \frac{1}{3\beta l_{Pl}^2} \left[ 1 - \left( 1 - \beta l_{Pl}^2 H^2 \right)^{\frac{3}{2}} \right] = \frac{8\pi G}{3} \rho, \quad (33)$$

where we have used  $A = 4\pi \tilde{r}_A^2$  (for more details about derivation of these equations, see Ref. [70]). Now, we assume the energy component of the universe to be a tachyon field  $\phi$  with potential  $V(\phi)$  and warp factor  $\lambda$  [56, 71]. In this case, the energy density and pressure are

$$\rho = \frac{V(\phi)}{\sqrt{1 - \lambda \dot{\phi}^2}}, \quad p = -V(\phi) \sqrt{1 - \lambda \dot{\phi}^2}, \quad (34)$$

leading to

$$\dot{H} \left( \frac{\beta l_{Pl}^2}{2} \right) \left( \frac{H^2}{1 - \sqrt{1 - \beta l_{Pl}^2 H^2}} \right) = -4\pi G \left( \frac{\lambda V \dot{\phi}^2}{\sqrt{1 - \lambda \dot{\phi}^2}} \right), \quad (35)$$

$$\frac{H^2}{2} + \frac{1}{3\beta l_{Pl}^2} \left[ 1 - \left( 1 - \beta l_{Pl}^2 H^2 \right)^{\frac{3}{2}} \right] = \frac{8\pi G}{3} \left( \frac{V}{\sqrt{1 - \lambda \dot{\phi}^2}} \right). \quad (36)$$

Note that, if we use the Friedmann equations (35) and (36) together with the conservation equation (11), we find that the effect of the minimal length doesn't show itself in the equation of motion of the tachyon field up to the first order in  $l_{Pl}^2$ . Therefore, we have

$$\frac{\lambda \ddot{\phi}}{1 - \lambda \dot{\phi}^2} + 3\lambda H \dot{\phi} + \frac{V'(\phi)}{V(\phi)} = 0, \quad (37)$$

as the equation of motion of the tachyon field. By these modified Friedmann equations, the inflation parameters are modified too. In the next section, we use these modified equations and study the inflation in the presence of the minimal length.

## 4 Tachyon Inflation in the Presence of the Minimal Length

To solve some problems of the standard model of cosmology, a primordial exponential phase of expansion in the early universe is needed. In an exponential phase of expansion, the Hubble parameter should be almost constant. This is because there was an end to the inflation and after that, the universe became radiation-dominated. In this way, some parameters for inflation have been defined which are called the slow-roll parameters. These parameters are defined as

$$\epsilon = -\frac{\dot{H}}{H^2}, \quad \eta = -\frac{\ddot{H}}{H\dot{H}}, \quad (38)$$

which in the inflation phase should satisfy the conditions  $|\epsilon, \eta| \ll 1$ . In the single field inflation models, the slow-roll conditions are corresponding to  $\dot{\phi}^2 \ll V(\phi)$  and  $\ddot{\phi} \ll 3H\dot{\phi}$ . Under these conditions, the Hubble parameter is almost constant ( $H^2 \simeq V(\phi)$ ) when the potential is sufficiently flat. Now, the slow-roll parameters in our model take the following forms

$$\epsilon \simeq \frac{\kappa^2 V'^2}{18 H^4 \lambda V} \left( 1 - \frac{\beta l_{Pl}^2 H^2}{16 \pi} - \frac{\beta^2 l_{Pl}^4 H^4}{256 \pi^2} \right)^{-1}, \quad (39)$$

$$\eta = \frac{\left[ -\frac{\kappa^2}{27} \frac{V'^2 V''}{2\dot{H} \lambda^2 H^4 V^2} - \epsilon \left( 1 - \frac{3\beta l_{Pl}^2 H^2}{16 \pi} - \frac{5\beta^2 l_{Pl}^4 H^4}{256 \pi^2} \right) \right]}{\left[ 1 - \frac{\beta l_{Pl}^2 H^2}{16 \pi} - \frac{\beta^2 l_{Pl}^4 H^4}{256 \pi^2} \right]}, \quad (40)$$

where we have used  $\kappa^2 = 8\pi G$  and the small limit of  $\beta$  as  $\beta \ll 4\pi H^2$ . We can also use the well-known e-folds number definition during the time interval between the Hubble crossing of the physical scales (*hc*) and the end of inflation (*end*) as

$$N = \int_{t_{hc}}^{t_{end}} H dt = \int_{\phi_{hc}}^{\phi_{end}} \frac{H}{\dot{\phi}} d\phi, \quad (41)$$

where the parameter  $H$  is given by equation (36). Now, we can study the perturbation parameters in this model to find more information about the effects of the presence of the minimal length in the theory. In the study of the perturbation parameters, the wave number plays an important role. When we consider the minimal length in the theory, the wave number gets modified. It has been shown that, by considering the uncertainly relation (6), the modified commutation relation is given by [19]

$$[X_i, P_j] = i \left( \delta_{ij} + \beta_{ijkl} l_{Pl}^2 p^k p^l \right). \quad (42)$$

Now, we can write the position and momentum operators in the position space as

$$X^i = x^i, \quad P^i = p^i (1 + \beta l_{Pl}^2 p^2). \quad (43)$$

According to the equation (43) and the relation  $p = k$  (since we have set  $\hbar = 1$ ), we find the modified wave number as [72]

$$K^i = k^i(1 + \beta l_{Pl}^2 k^2). \quad (44)$$

With this modified wave number, some perturbation parameters get modified too. The first important parameter that we study here is the scalar spectral index which is now defined as

$$n_s = 1 + \frac{d \ln \mathcal{A}_s}{d \ln k(1 + \beta l_{Pl}^2 k^2)} \cong 1 + (1 + \beta l_{Pl}^2 k^2) \frac{d \ln \mathcal{A}_s}{d \ln k} = 1 + (1 + \beta l_{Pl}^2 k^2) (-2\epsilon - \eta - s), \quad (45)$$

where  $\mathcal{A}_s$  is the amplitude of the scalar perturbations defined as

$$\mathcal{A}_s = \frac{H^4}{4\pi^2 V (1 - c_s^2)}, \quad (46)$$

Note that, the effect of the minimal length in the amplitude is encoded in  $H$ . The parameter  $c_s$  in equation (46) is the sound speed given by

$$c_s = \sqrt{1 - \dot{\phi}^2}. \quad (47)$$

Also, the parameter  $s$  is defined as

$$s = \frac{1}{H} \frac{\dot{c}_s}{c_s}, \quad (48)$$

The tensor spectral index in the presence of the minimal length is given by

$$n_T = \frac{d \ln \mathcal{A}_T}{d \ln k(1 + \beta l_{Pl}^2 k^2)} \cong (1 + \beta l_{Pl}^2 k^2) \frac{d \ln \mathcal{A}_T}{d \ln k} = -(1 + \beta l_{Pl}^2 k^2) (2\epsilon), \quad (49)$$

where  $\mathcal{A}_T$  is the amplitude of the tensor perturbations that is defined as

$$\mathcal{A}_T = \frac{2\kappa^2 H^2}{\pi^2}. \quad (50)$$

Finally, the tensor-to-scalar ratio is given by

$$r = \frac{\mathcal{A}_T}{\mathcal{A}_s} = 16 c_s \epsilon = -\frac{8c_s}{1 + \beta l_{Pl}^2 k^2} n_T \quad (51)$$

This shows that the consistency relation gets modified in this framework due to existence of a minimal measurable length. Now, we are in the position that we can test our model's viability in confrontation with recent observational data. We perform our numerical analysis by choosing power-law, inverse power-law and inverse exponential potentials.

## 5 Observational Viability of the Model

When we consider a simple tachyon field with quadratic potential, there is no consistency between the model and Planck2018 TT, TE, EE+lowE+lensing+BAO+BK14 observational data.

For instance, the value of the tensor-to-scalar ratio in the tachyon model with  $\phi^2$  and  $\phi^4$  potentials for both  $N = 50$  and  $N = 60$  is larger than the constraint released by Planck2018 TT, TE, EE+lowE+lensing+BAO+BK14 data. The observational upper bound on the tensor-to-scalar ratio, based on  $\Lambda$ CDM+ $r+\frac{dn_s}{d \ln k}$  model, is  $r < 0.072$  [60, 61]. Planck2018 TT, TE, EE+lowE+lensing+BAO+BK14 data implies the constraint on the scalar spectral index as  $n_s = 0.9658 \pm 0.0038$  [60, 61]. In this regard, the  $r - n_s$  plot for the tachyon model with  $\phi^2$ -potential lies beyond the observational confidence levels and makes the model less favorable. Also, Planck2018 TT, TE, EE+lowE+lensing+BAO+BK18 data implies a tighter constraint on the tensor-to-scalar ratio ( $r < 0.036$  at 95% CL [62, 63]) that rules out the tachyon inflation with  $\phi^2$  and  $\phi^4$  potentials. Now that we consider the minimal length in the tachyon model, by considering the fact that it changes the slow-roll parameters and therefore the perturbation parameters of the tachyon model, we wonder if it is possible to find any consistency between the tachyon model with quadratic potential and observational data. In this regard, we assume  $V = \frac{1}{2} m^2 \phi^2$  and  $V = \frac{v}{4} \phi^4$  potentials, where  $m = 1.4 \times 10^{13}$  GeV and  $v = 1.4 \times 10^{-13}$  [73]. By these potentials, we find the slow-roll parameters (39) and (40) in terms of the model's parameters. Then, we substitute these parameters in the perturbations parameters  $n_s$ ,  $n_T$ , and  $r$ . To perform the numerical analysis, it is better to express the scalar field in terms of other parameters. To this end, by using equations (36), (37) and (41), we find the scalar field at horizon crossing in terms of  $N$  and  $\beta$ . In this way, we obtain the slow-roll parameters and therefore the perturbations parameters in terms of  $N$  and  $\beta$ . In this situation, it is possible to test the observational viability of the model. Figure 1 shows  $r - n_s$  behavior in the tachyon model with  $\phi^2$  and  $\phi^4$  potentials, in the presence of the minimal length. As the figure shows, the presence of the minimal length makes the tachyon inflation model observationally viable. Of course, there are some constraints on  $\beta$  that lead to the consistency of the model with observational data. To plot this figure, we have adopted  $N = 60$  and  $0.8 < \lambda \leq 1$ . Note that, in the full numerical analysis, we have adopted  $0 < \lambda \leq 1$ . However, in plotting the figure, we consider a smaller range of  $\lambda$ , just to show the  $r - n_s$  behavior in confrontation with several data. As this figure shows,  $r - n_s$  plot in our model with  $\phi^2$  potential, in two ranges of the parameter  $\beta$  is consistent with Planck2018 TT, TE, EE +lowE+lensing+BK14 +BAO data. When we consider Planck2018 TT, TE, EE +lowE+lensing+BK18 +BAO data, only one range of the model's parameters makes the model consistent with observation. We have also performed the same analysis with  $\phi^4$  potential. In tables 1-4, we have presented the observationally viable ranges of  $\beta$ , for some sample values of  $\lambda$  as  $\lambda = 0.1, 0.4, 0.7$  and 1 and for both of the mentioned potentials.

The behavior of the tensor-to-scalar ratio versus the tensor spectral index, in the background of both Planck2018 TT, TE, EE +lowE+lensing+BK14+BAO +LIGO and Virgo2016 and Planck2018 TT, TE, EE +lowE+lensing+BK18+BAO +LIGO and Virgo2016 data is shown in figure 2. As this figure shows,  $r - n_T$  of our model in some subspaces of the model's parameter space is observationally viable. In this case also, the observationally viable ranges of  $\beta$ , for some sample values of  $\lambda$  are shown in tables 1- 4. To demonstrate the constraints on the model's parameters more clearly, in figures 3 and 4 we have plotted  $\lambda - \beta$  space in confrontation with the observationally viable ranges of  $r - n_s$  and  $r - n_T$ .

Other classes of potentials for the tachyon field, motivated by string theory, are inverse power-law and inverse exponential potentials. Tachyon inflation with these potentials has already been studied in [54], where the authors have used Planck2015 datasets. By comparing their results with new observational data, we find out that there is no consistency between the tachyon inflation with

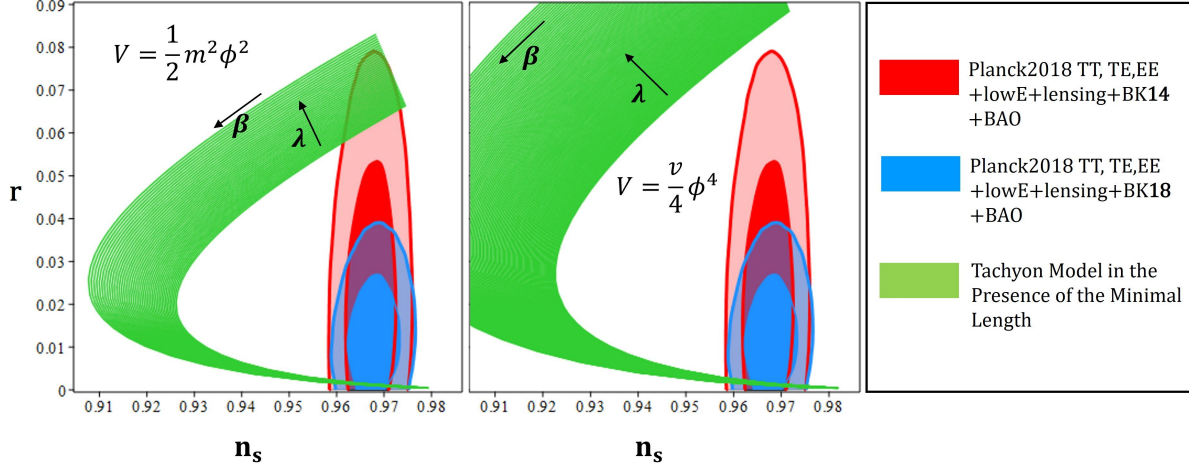


Figure 1: Tensor-to-scalar ratio versus the scalar spectral index for the tachyon inflation with  $\phi^2$  and  $\phi^4$  potentials in the presence of a minimal measurable length, in the background of Planck2018 TT, TE, EE +lowE+lensing+BK14+BAO and Planck2018 TT, TE, EE +lowE+lensing+BK18+BAO data. The arrows show the direction where the parameters increase.

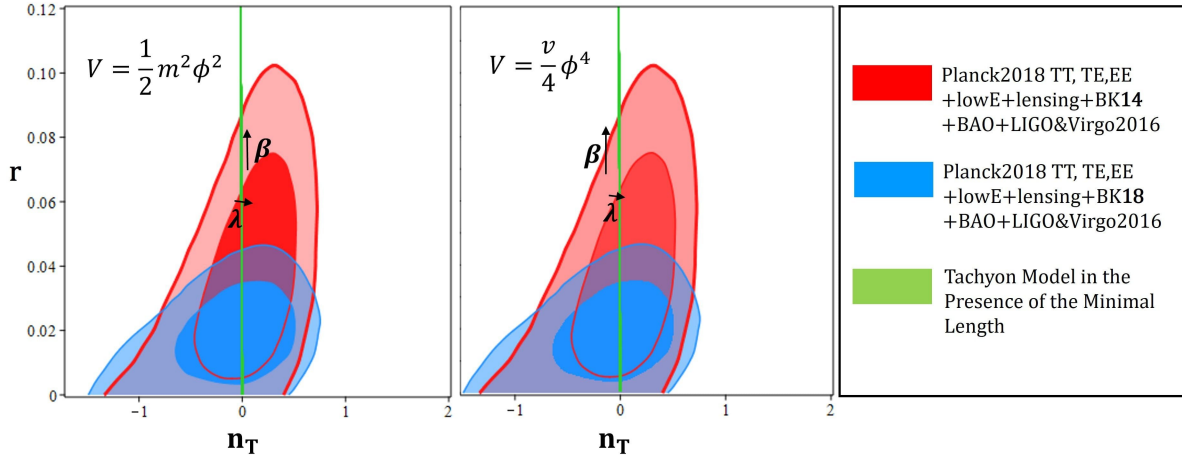


Figure 2: Tensor-to-scalar ratio versus the tensor spectral index for the tachyon inflation with  $\phi^2$  and  $\phi^4$  potentials in the presence of a minimal measurable length, in the background of Planck2018 TT, TE, EE +lowE+lensing+BK14+BAO+LIGO and Virgo2016 and Planck2018 TT, TE, EE +lowE+lensing+BK18+BAO+LIGO and Virgo2016 data. The arrows show the direction where the parameters increase.

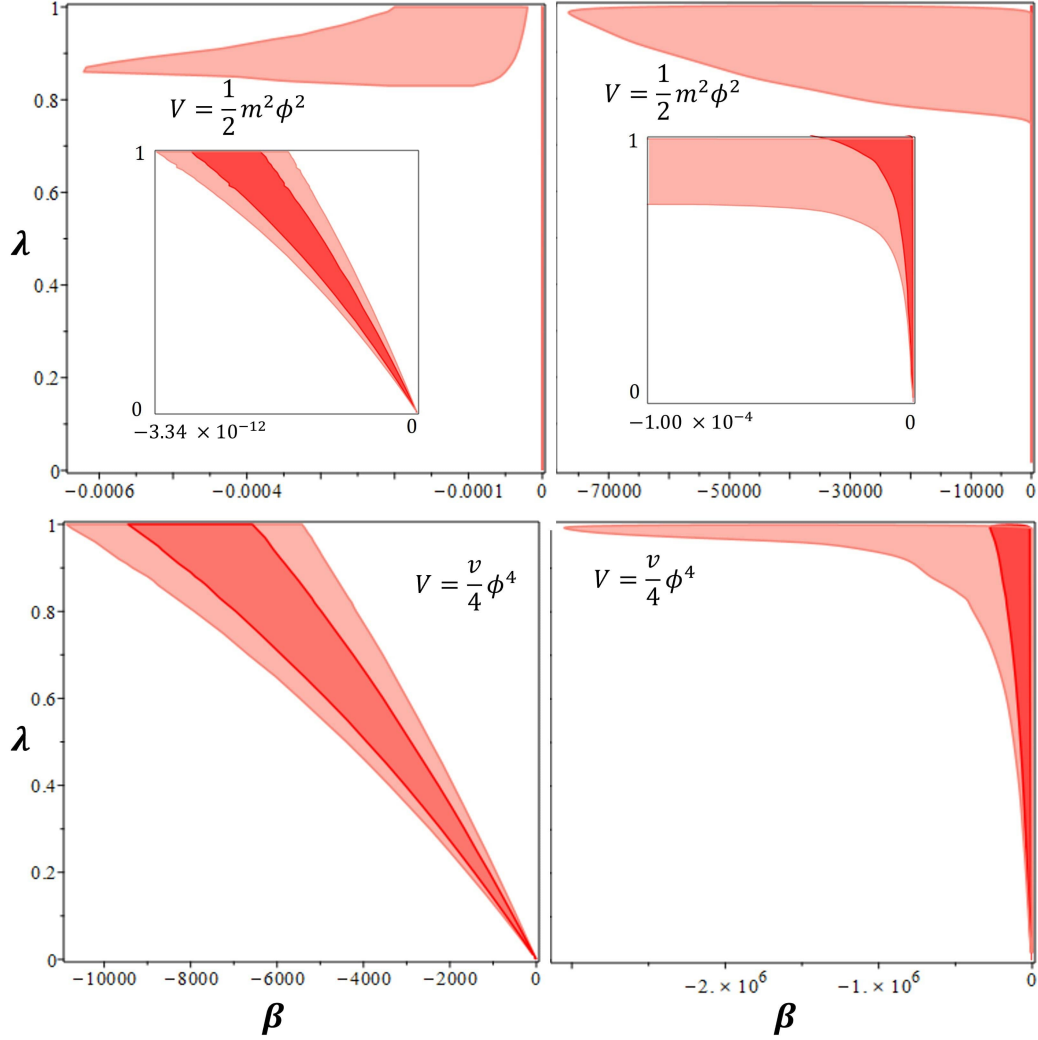


Figure 3: Left panels: ranges of the parameters  $\lambda$  and  $\beta$  for the tachyon inflation in the presence of a minimal length, leading to observationally viable values of  $r - n_s$ , in confrontation with Planck2018 TT, TE, and EE+lowE+lensing+BAO+BK14 data at 68% CL (dark red) and 95% CL (light red). Right panels: ranges of the parameters  $\lambda$  and  $\beta$  for the tachyon inflation in the presence of the minimal length, leading to observationally viable values of  $r - n_T$ , in confrontation with Planck2018 TT, TE, and EE+lowE+lensing+BK14+BAO+LIGO and Virgo2016 data at 68% CL (dark red) and 95% CL (light red).

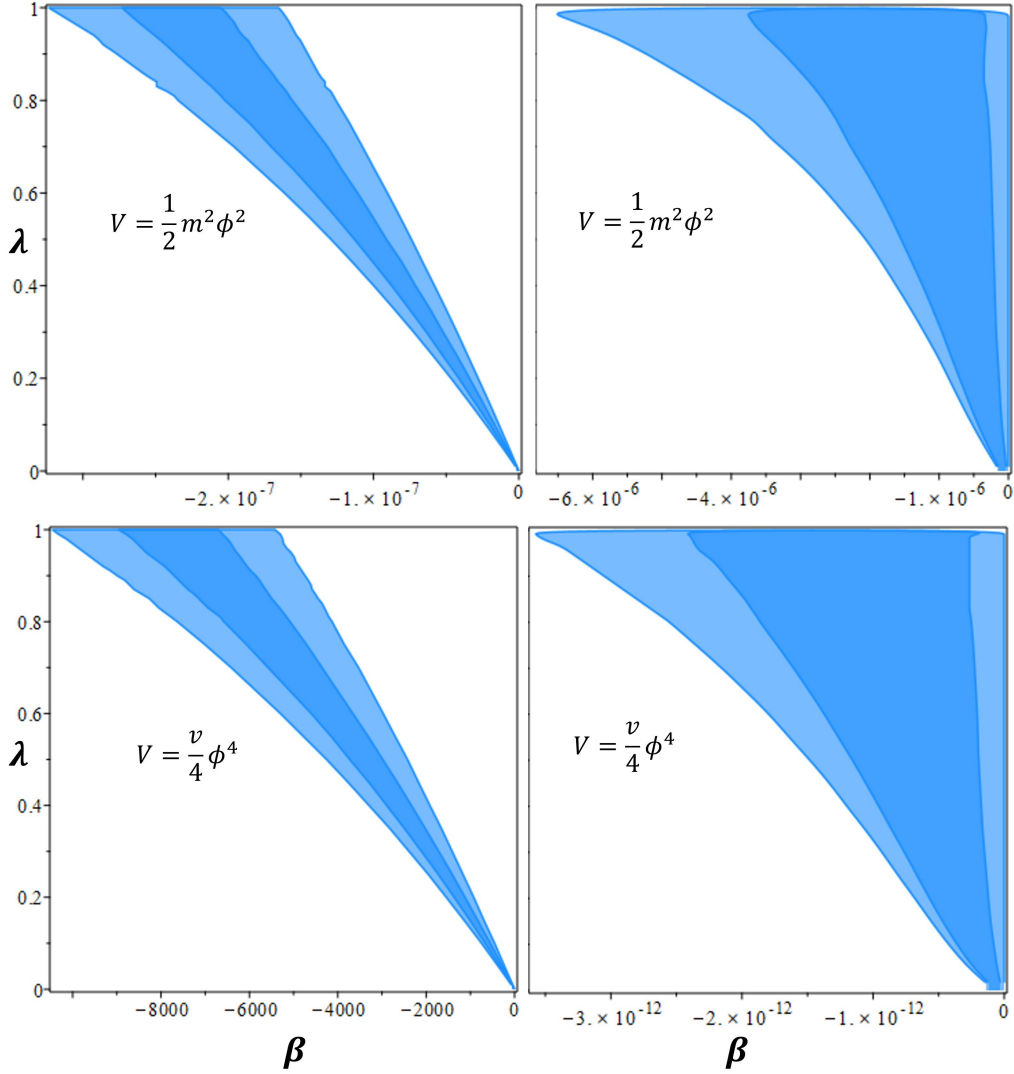


Figure 4: Left panels: ranges of the parameters  $\lambda$  and  $\beta$  for the tachyon inflation in the presence of a minimal length, leading to observationally viable values of  $r - n_s$ , in confrontation with Planck2018 TT, TE, and EE+lowE+lensing+BAO+BK18 data at 68% CL (dark blue) and 95% CL (light blue). Right panels: ranges of the parameters  $\lambda$  and  $\beta$  for the tachyon inflation in the presence of the minimal length, leading to observationally viable values of  $r - n_T$ , in confrontation with Planck2018 TT, TE, and EE+lowE+lensing+BK18+BAO+LIGO and Virgo2016 data at 68% CL (dark blue) and 95% CL (light blue).

Table 1: Ranges of the parameter  $\beta$  in which the tensor-to-scalar ratio, scalar spectral index and tensor spectral index of the tachyon model with  $\phi^2$  potential in the presence of a minimal length are consistent with different joint data sets.

	Planck2018 TT,TE,EE+lowE +lensing+BK14+BAO	Planck2018 TT,TE,EE+lowE +lensing+BK14+BAO	Planck2018 TT,TE,EE+lowE lensing+BK14+BAO +LIGO&Virgo2016	Planck2018 TT,TE,EE+lowE lensing+BK14+BAO LIGO&Virgo2016
$\lambda$	68% CL	95% CL	68% CL	95% CL
0.1	$-2.10 \times 10^{-8} < \beta < -1.60 \times 10^{-8}$	$-2.33 \times 10^{-8} < \beta < -1.37 \times 10^{-8}$	$-6.60 \times 10^{-7} < \beta < -1.39 \times 10^{-9}$	$-8.34 \times 10^{-7} < \beta < 0$
0.4	$-9.27 \times 10^{-8} < \beta < -6.95 \times 10^{-8}$	$-1.03 \times 10^{-7} < \beta < -5.80 \times 10^{-8}$	$-2.34 \times 10^{-6} < \beta < -2.95 \times 10^{-9}$	$-3.82 \times 10^{-6} < \beta < 0$
0.7	$-1.79 \times 10^{-7} < \beta < -1.29 \times 10^{-7}$	$-2.03 \times 10^{-7} < \beta < -1.08 \times 10^{-7}$	$-6.26 \times 10^{-6} < \beta < -4.00 \times 10^{-9}$	$-3.13 \times 10^{-5} < \beta < 0$
1	$-2.90 \times 10^{-7} < \beta < -2.01 \times 10^{-7}$	$-3.35 \times 10^{-7} < \beta < -1.65 \times 10^{-7}$ $-2.00 \times 10^{-4} < \beta < -2.00 \times 10^{-5}$	$-5.21 \times 10^{-5} < \beta < -5.21 \times 10^{-9}$	$-7.82 \times 10^4 < \beta < 0$

Table 2: Ranges of the parameter  $\beta$  in which the tensor-to-scalar ratio, scalar spectral index and tensor spectral index of the tachyon model with  $\phi^4$  potential in the presence of a minimal length are consistent with different joint data sets.

	Planck2018 TT,TE,EE+lowE +lensing+BK14+BAO	Planck2018 TT,TE,EE+lowE +lensing+BK14+BAO	Planck2018 TT,TE,EE+lowE lensing+BK14+BAO +LIGO&Virgo2016	Planck2018 TT,TE,EE+lowE lensing+BK14+BAO LIGO&Virgo2016
$\lambda$	68% CL	95% CL	68% CL	95% CL
0.1	$-6.97 \times 10^2 < \beta < -5.33 \times 10^2$	$-7.72 \times 10^2 < \beta < -4.56 \times 10^2$	$-1.84 \times 10^4 < \beta < -4.18 \times 10^2$	$-2.30 \times 10^4 < \beta < 0$
0.4	$-3.03 \times 10^3 < \beta < -2.26 \times 10^3$	$-3.39 \times 10^3 < \beta < -1.92 \times 10^3$	$-5.85 \times 10^4 < \beta < -9.06 \times 10^2$	$-8.36 \times 10^4 < \beta < 0$
0.7	$-5.89 \times 10^3 < \beta < -4.23 \times 10^3$	$-6.65 \times 10^3 < \beta < -3.55 \times 10^3$	$-1.23 \times 10^5 < \beta < -1.28 \times 10^3$	$-2.43 \times 10^5 < \beta < 0$
1	$-9.44 \times 10^3 < \beta < -6.57 \times 10^3$	$-1.08 \times 10^4 < \beta < -5.42 \times 10^3$	$-2.82 \times 10^5 < \beta < -1.49 \times 10^3$	$-3.11 \times 10^6 < \beta < 0$

Table 3: Ranges of the parameter  $\beta$  in which the tensor-to-scalar ratio, scalar spectral index and tensor spectral index of the tachyon model with  $\phi^2$  potential in the presence of a minimal length are consistent with different joint data sets.

	Planck2018 TT,TE,EE+lowE +lensing+BK18+BAO	Planck2018 TT,TE,EE+lowE +lensing+BK18+BAO	Planck2018 TT,TE,EE+lowE lensing+BK18+BAO +LIGO&Virgo2016	Planck2018 TT,TE,EE+lowE lensing+BK18+BAO LIGO&Virgo2016
$\lambda$	68% CL	95% CL	68% CL	95% CL
0.1	$-2.00 \times 10^{-8} < \beta < -1.66 \times 10^{-8}$	$-2.26 \times 10^{-8} < \beta < -1.37 \times 10^{-8}$	$-4.40 \times 10^{-7} < \beta < -9.56 \times 10^{-9}$	$-5.21 \times 10^{-7} < \beta < 0$
0.4	$-8.74 \times 10^{-8} < \beta < -7.11 \times 10^{-8}$	$-9.98 \times 10^{-8} < \beta < -5.80 \times 10^{-8}$	$-1.23 \times 10^{-6} < \beta < -1.98 \times 10^{-8}$	$-1.61 \times 10^{-6} < \beta < 0$
0.7	$-1.70 \times 10^{-7} < \beta < -1.31 \times 10^{-7}$	$-1.96 \times 10^{-7} < \beta < -1.07 \times 10^{-7}$	$-2.7 \times 10^{-6} < \beta < -2.60 \times 10^{-8}$	$-3.28 \times 10^{-6} < \beta < 0$
1	$-2.73 \times 10^{-7} < \beta < -2.05 \times 10^{-7}$	$-2.49 \times 10^{-7} < \beta < -1.65 \times 10^{-7}$	$-3.82 \times 10^{-6} < \beta < -3.13 \times 10^{-8}$	$-6.78 \times 10^{-6} < \beta < 0$

Table 4: Ranges of the parameter  $\beta$  in which the tensor-to-scalar ratio, scalar spectral index and tensor spectral index of the tachyon model with  $\phi^4$  potential in the presence of a minimal length are consistent with different joint data sets.

	Planck2018 TT,TE,EE+lowE +lensing+BK18+BAO	Planck2018 TT,TE,EE+lowE +lensing+BK18+BAO	Planck2018 TT,TE,EE+lowE lensing+BK18+BAO +LIGO&Virgo2016	Planck2018 TT,TE,EE+lowE lensing+BK18+BAO LIGO&Virgo2016
$\lambda$	68% CL	95% CL	68% CL	95% CL
0.1	$-6.64 \times 10^2 < \beta < -5.48 \times 10^2$	$-7.45 \times 10^2 < \beta < -4.51 \times 10^2$	$-1.25 \times 10^4 < \beta < -2.78 \times 10^2$	$-1.48 \times 10^4 < \beta < 0$
0.4	$-2.89 \times 10^3 < \beta < -2.33 \times 10^3$	$-3.29 \times 10^3 < \beta < -1.91 \times 10^3$	$-3.32 \times 10^4 < \beta < -6.09 \times 10^2$	$-4.18 \times 10^4 < \beta < 0$
0.7	$-5.57 \times 10^3 < \beta < -4.35 \times 10^3$	$-6.41 \times 10^3 < \beta < -3.53 \times 10^3$	$-5.59 \times 10^4 < \beta < -7.84 \times 10^2$	$-7.49 \times 10^4 < \beta < 0$
1	$-8.95 \times 10^3 < \beta < -6.69 \times 10^3$	$-1.04 \times 10^4 < \beta < -5.42 \times 10^3$	$-8.57 \times 10^4 < \beta < -9.23 \times 10^2$	$-1.25 \times 10^5 < \beta < 0$

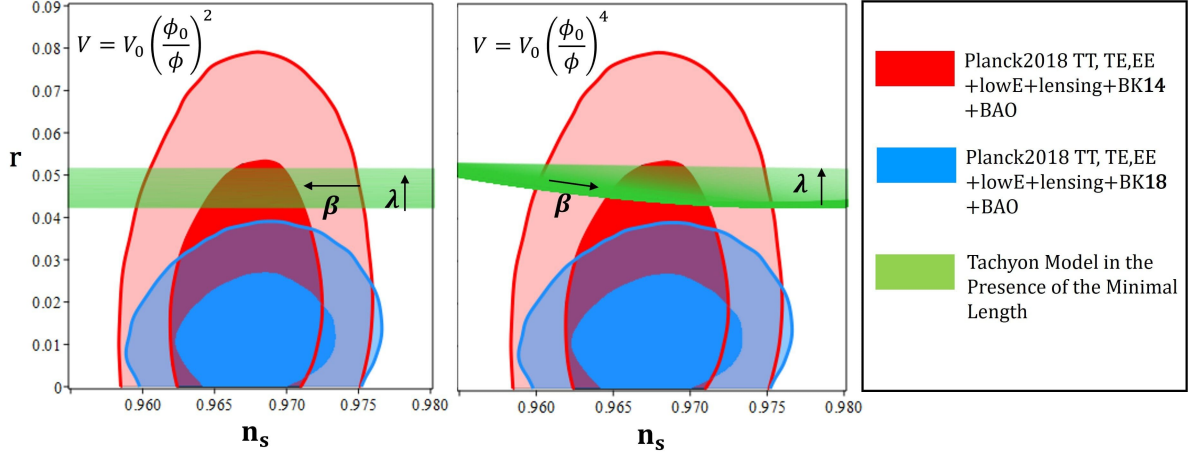


Figure 5: Tensor-to-scalar ratio versus the scalar spectral index for the tachyon inflation with  $\phi^{-2}$  and  $\phi^{-4}$  potentials in the presence of a minimal measurable length, in the background of Planck2018 TT, TE, EE +lowE+lensing+BK14+BAO and Planck2018 TT, TE, EE +lowE+lensing+BK18+BAO data. The arrows show the direction where the parameters increase.

these potentials and observational data. Now, we are going to check if we can find any observational viability of the tachyon inflation with inverse power-law and inverse exponential potentials in the presence of the minimal length. In this regard, we first consider  $V = V_0 \left(\frac{\phi_0}{\phi}\right)^2$  and  $V = V_0 \left(\frac{\phi_0}{\phi}\right)^4$ , where  $V_0$  and  $\phi_0$  are some constants (re-scaled to 1). We follow the structure for the  $\phi^2$  and  $\phi^4$  potentials and perform some numerical analysis on our model. The behavior of  $r - n_s$  for the tachyon model with  $\phi^{-2}$  and  $\phi^{-4}$  potentials has been shown in figure 5. As we can see from this figure, the tachyon inflation with both considered potentials are only consistent with Planck2018 TT, TE, EE +lowE+lensing+BK14+BAO data at 68% CL and 95% CL. However,  $r - n_T$  plots are consistent with both Planck2018 TT, TE, EE +lowE+lensing+BK14+BAO and Planck2018 TT, TE, EE +lowE+lensing+BK18+BAO data (figure 6). For some sample values of  $\lambda$ , we have obtained constraints on  $\beta$ , summarized in tables 5-8. Also, in figures 7 and 8 we have plotted  $\lambda - \beta$  space in confrontation with the observationally viable ranges of  $r - n_s$  and  $r - n_T$ . It should be noticed that, with  $\phi^{-2}$  potential, the model has numerical results only for  $\lambda > 0.68$ .

Now, we consider the inverse exponential potential as  $V = V_0 \exp(-\frac{\phi}{\phi_0})$ , where again  $V_0$  and  $\phi_0$  are some constants that we re-scale them to 1. Similar to the previous potentials, we perform numerical analysis on the  $r - n_s$  and  $r - n_T$ . The results are shown in figures 9 and 10. As we see from these figures, in this case also,  $r - n_s$  is only consistent with Planck2018 TT, TE, EE +lowE+lensing+BK14+BAO data at 95% CL. However,  $r - n_T$  is consistent with both Planck2018 TT, TE, EE +lowE+lensing+BK14+BAO+LIGO and Virgo2016 and Planck2018 TT, TE, EE +lowE+lensing+BK18+BAO+LIGO and Virgo2016 data. As before, we obtained some constraints on  $\beta$  for some sample values of  $\lambda$ , summarized in tables 9 and 10. Figures 11 and 12 demonstrate  $\lambda - \beta$  space in confrontation with the observationally viable ranges of  $r - n_s$  and  $r - n_T$  for the model with inverse exponential potential.

Note that, the warp factor  $\lambda$  is not enough itself to make the tachyon model observationally

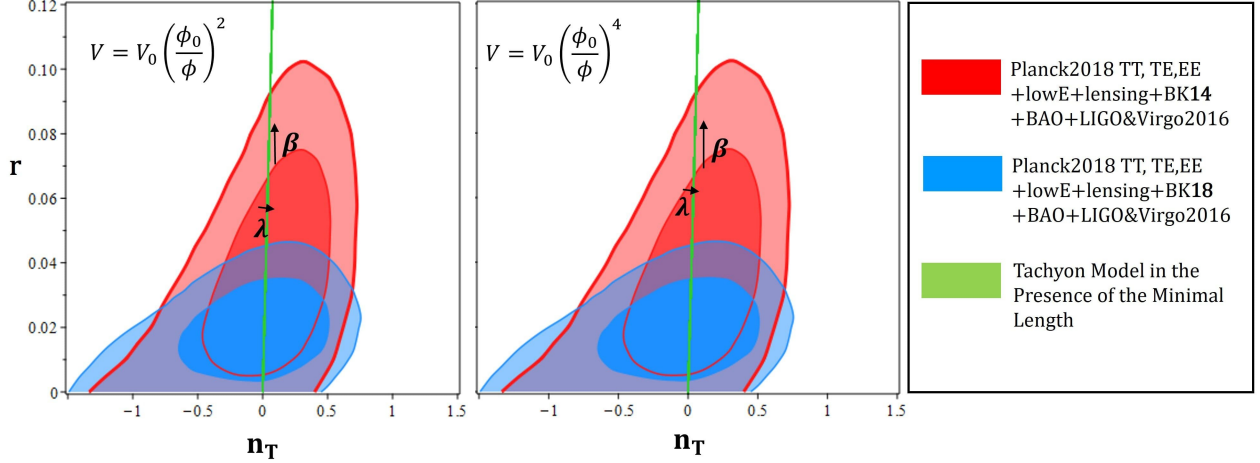


Figure 6: Tensor-to-scalar ratio versus the tensor spectral index for the tachyon inflation with  $\phi^{-2}$  and  $\phi^{-4}$  potentials in the presence of a minimal measurable length, in the background of Planck2018 TT, TE, EE +lowE+lensing+BK14+BAO+LIGO and Virgo2016 and Planck2018 TT, TE, EE +lowE+lensing+BK18+BAO+LIGO and Virgo2016 data. The arrows show the direction where the parameters increase.

Table 5: Ranges of the parameter  $\beta$  in which the tensor-to-scalar ratio, scalar spectral index and tensor spectral index of the tachyon model with  $\phi^{-2}$  potential in the presence of a minimal length are consistent with different joint data sets.

	Planck2018 TT,TE,EE+lowE +lensing+BK14+BAO	Planck2018 TT,TE,EE+lowE +lensing+BK14+BAO	Planck2018 TT,TE,EE+lowE lensing+BK14+BAO +LIGO&Virgo2016	Planck2018 TT,TE,EE+lowE lensing+BK14+BAO LIGO&Virgo2016
$\lambda$	68% CL	95% CL	68% CL	95% CL
0.7	$-1.05 \times 10^{-1} < \beta < -1.04 \times 10^{-1}$	$-1.06 \times 10^{-1} < \beta < -1.03 \times 10^{-1}$	$-1.96 \times 10^{-1} < \beta < -1.44 \times 10^{-1}$	$-2.21 \times 10^{-1} < \beta < 0$
0.8	$-1.07 \times 10^{-1} < \beta < -1.05 \times 10^{-1}$	$-1.08 \times 10^{-1} < \beta < -1.03 \times 10^{-1}$	$-2.40 \times 10^{-1} < \beta < -1.07 \times 10^{-1}$	$-2.48 \times 10^{-1} < \beta < 0$
0.9	$-2.31 \times 10^{-1} < \beta < -1.10 \times 10^{-1}$	$-1.56 < \beta < -1.13 \times 10^{-1}$	$-5.44 \times 10^{-1} < \beta < -2.49 \times 10^{-1}$	$-3.30 < \beta < 0$
1	$-4.56 < \beta < -5.53 \times 10^{-1}$	$-45.5 < \beta < -1.14 \times 10^{-1}$	$-10.6 < \beta < -0.601$	$-104 < \beta < 0$

Table 6: Ranges of the parameter  $\beta$  in which the tensor-to-scalar ratio, scalar spectral index and tensor spectral index of the tachyon model with  $\phi^{-4}$  potential in the presence of a minimal length are consistent with different joint data sets.

	Planck2018 TT,TE,EE+lowE +lensing+BK14+BAO	Planck2018 TT,TE,EE+lowE +lensing+BK14+BAO	Planck2018 TT,TE,EE+lowE lensing+BK14+BAO +LIGO&Virgo2016	Planck2018 TT,TE,EE+lowE lensing+BK14+BAO LIGO&Virgo2016
$\lambda$	68% CL	95% CL	68% CL	95% CL
0.1	$-1.94 \times 10^{-7} < \beta < -1.25 \times 10^{-7}$	$-2.45 \times 10^{-7} < \beta < -8.10 \times 10^{-8}$	$-1.95 \times 10^{-4} < \beta < -1.24 \times 10^{-7}$	$-2.47 \times 10^{-6} < \beta < 0$
0.4	$-3.10 \times 10^{-6} < \beta < -2.01 \times 10^{-6}$	$-3.90 \times 10^{-6} < \beta < -1.31 \times 10^{-6}$	$-3.10 \times 10^{-5} < \beta < -2.01 \times 10^{-6}$	$-3.87 \times 10^{-5} < \beta < 0$
0.7	$-9.50 \times 10^{-6} < \beta < -6.12 \times 10^{-6}$	$-1.20 \times 10^{-5} < \beta < -4.00 \times 10^{-6}$	$-9.45 \times 10^{-5} < \beta < -6.07 \times 10^{-6}$	$-1.16 \times 10^{-4} < \beta < 0$
1	$-1.93 \times 10^{-5} < \beta < -1.26 \times 10^{-5}$	$-2.45 \times 10^{-5} < \beta < -8.15 \times 10^{-6}$	$-1.90 \times 10^{-4} < \beta < -1.26 \times 10^{-5}$	$-2.48 \times 10^{-4} < \beta < 0$

Table 7: Ranges of the parameter  $\beta$  in which the tensor-to-scalar ratio, scalar spectral index and tensor spectral index of the tachyon model with  $\phi^{-2}$  potential in the presence of a minimal length are consistent with different joint data sets.

	Planck2018 TT,TE,EE+lowE +lensing+BK18+BAO	Planck2018 TT,TE,EE+lowE +lensing+BK18+BAO	Planck2018 TT,TE,EE+lowE lensing+BK18+BAO +LIGO&Virgo2016	Planck2018 TT,TE,EE+lowE lensing+BK18+BAO LIGO&Virgo2016
$\lambda$	68% CL	95% CL	68% CL	95% CL
0.7	Not Consistent	Not Consistent	$-1.84 \times 10^{-1} < \beta < -1.49 \times 10^{-1}$	$-2.09 \times 10^{-1} < \beta < 0$
0.8	Not Consistent	Not Consistent	$-2.16 \times 10^{-1} < \beta < -1.11 \times 10^{-1}$	$-2.37 \times 10^{-1} < \beta < 0$
0.9	Not Consistent	Not Consistent	$-4.72 \times 10^{-1} < \beta < -2.57 \times 10^{-1}$	$-2.71 < \beta < 0$
1	Not Consistent	Not Consistent	$-9.75 < \beta < -4.32 \times 10^{-1}$	$-95.6 < \beta < 0$

Table 8: Ranges of the parameter  $\beta$  in which the tensor-to-scalar ratio, scalar spectral index and tensor spectral index of the tachyon model with  $\phi^{-4}$  potential in the presence of a minimal length are consistent with different joint data sets.

	Planck2018 TT,TE,EE+lowE +lensing+BK18+BAO	Planck2018 TT,TE,EE+lowE +lensing+BK18+BAO	Planck2018 TT,TE,EE+lowE lensing+BK18+BAO +LIGO&Virgo2016	Planck2018 TT,TE,EE+lowE lensing+BK18+BAO LIGO&Virgo2016
$\lambda$	68% CL	95% CL	68% CL	95% CL
0.1	Not Consistent	Not Consistent	$-5.82 \times 10^{-7} < \beta < -3.75 \times 10^{-8}$	$-7.35 \times 10^{-7} < \beta < 0$
0.4	Not Consistent	Not Consistent	$-9.30 \times 10^{-6} < \beta < -6.03 \times 10^{-7}$	$-1.17 \times 10^{-5} < \beta < 0$
0.7	Not Consistent	Not Consistent	$-2.85 \times 10^{-5} < \beta < -1.83 \times 10^{-6}$	$-3.60 \times 10^{-5} < \beta < 0$
1	Not Consistent	Not Consistent	$-5.79 \times 10^{-5} < \beta < -3.78 \times 10^{-6}$	$-7.35 \times 10^{-5} < \beta < 0$

Table 9: Ranges of the parameter  $\beta$  in which the tensor-to-scalar ratio, scalar spectral index and tensor spectral index of the tachyon model with  $\exp\left(-\frac{\phi}{\phi_0}\right)$  potential in the presence of a minimal length are consistent with different joint data sets.

	Planck2018 TT,TE,EE+lowE +lensing+BK14+BAO	Planck2018 TT,TE,EE+lowE +lensing+BK14+BAO	Planck2018 TT,TE,EE+lowE lensing+BK14+BAO +LIGO&Virgo2016	Planck2018 TT,TE,EE+lowE lensing+BK14+BAO LIGO&Virgo2016
$\lambda$	68% CL	95% CL	68% CL	95% CL
0.1	Not Consistent	$-5.50 \times 10^{-3} < \beta < -2.20 \times 10^{-8}$	$-8.25 \times 10^{-3} < \beta < -1.74 \times 10^{-8}$	$-9.90 \times 10^{-3} < \beta < 0$
0.4	Not Consistent	$-2.20 \times 10^{-2} < \beta < -9.10 \times 10^{-8}$	$-3.41 \times 10^{-2} < \beta < -7.46 \times 10^{-8}$	$-3.96 \times 10^{-2} < \beta < 0$
0.7	Not Consistent	$-3.86 \times 10^{-2} < \beta < -1.59 \times 10^{-7}$	$-5.98 \times 10^{-2} < \beta < -1.34 \times 10^{-7}$	$-6.94 \times 10^{-2} < \beta < 0$
1	Not Consistent	$-5.53 \times 10^{-2} < \beta < -2.30 \times 10^{-7}$	$-8.57 \times 10^{-2} < \beta < -1.02 \times 10^{-7}$	$-9.95 \times 10^{-2} < \beta < 0$

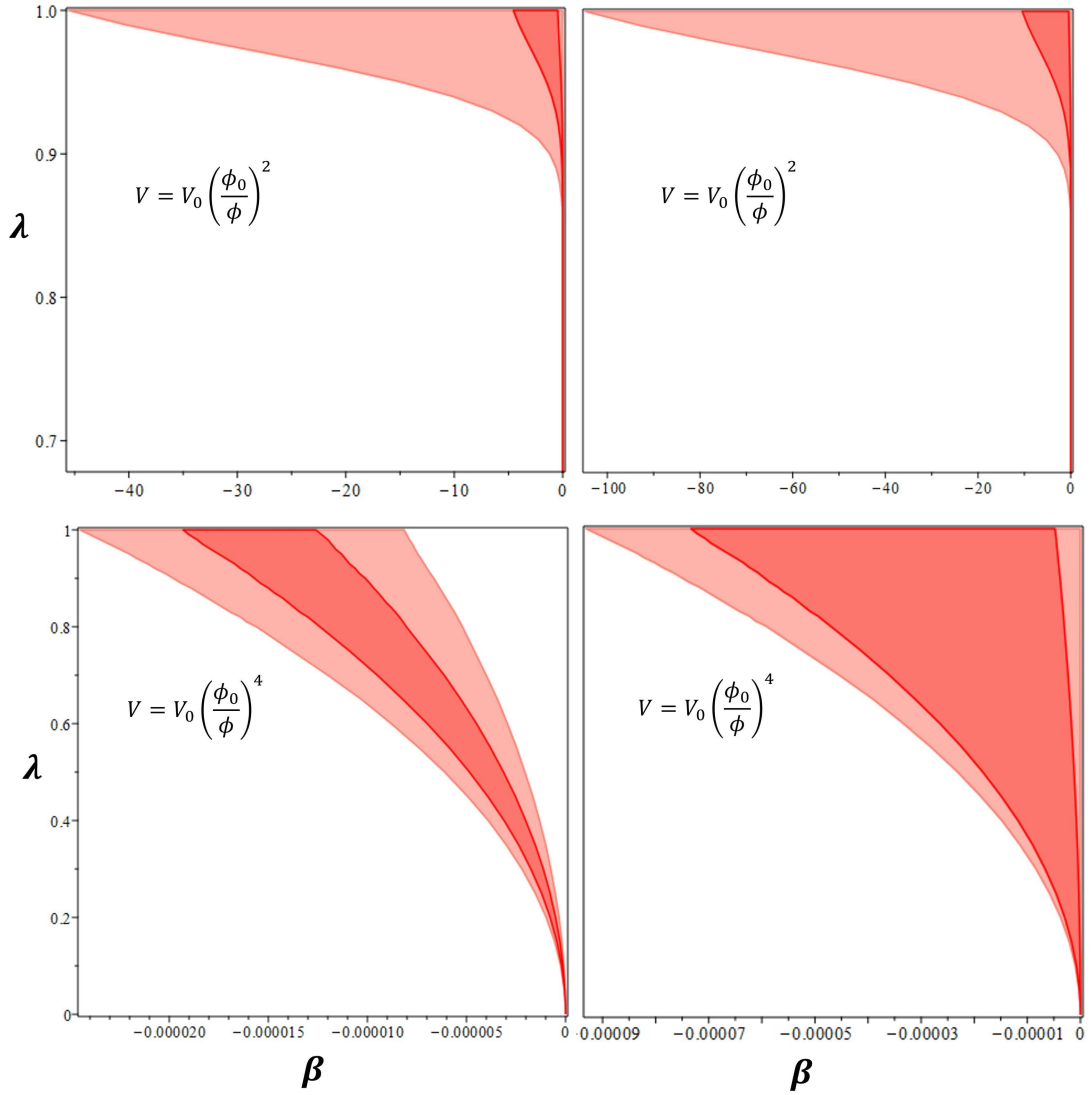


Figure 7: Left panels: ranges of the parameters  $\lambda$  and  $\beta$  for the tachyon inflation in the presence of a minimal length, leading to observationally viable values of  $r - n_s$ , in confrontation with Planck2018 TT, TE, and EE+lowE+lensing+BAO+BK14 data at 68% CL (dark red) and 95% CL (light red). Right panels: ranges of the parameters  $\lambda$  and  $\beta$  for the tachyon inflation in the presence of the minimal length, leading to observationally viable values of  $r - n_T$ , in confrontation with Planck2018 TT, TE, and EE+lowE+lensing+BK14+BAO+LIGO and Virgo2016 data at 68% CL (dark red) and 95% CL (light red).

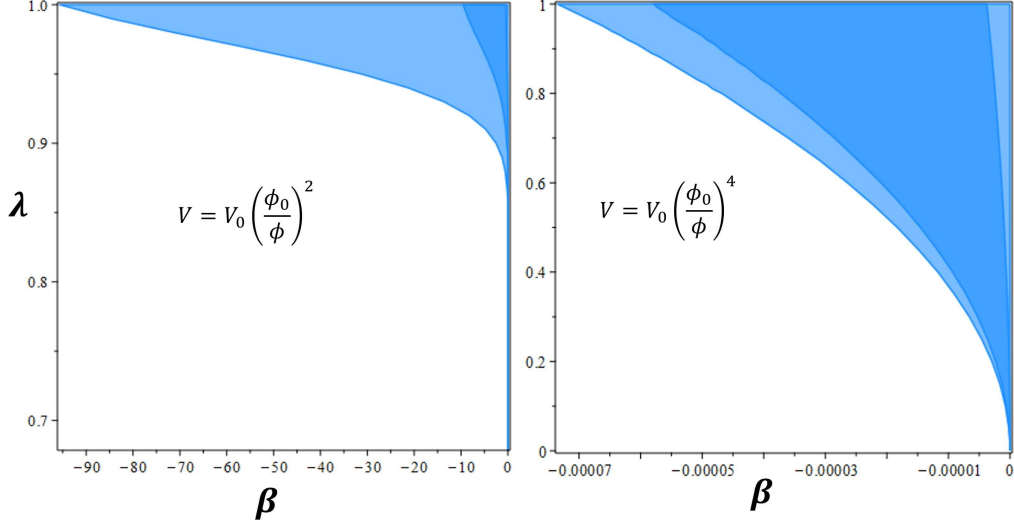


Figure 8: Ranges of the parameters  $\lambda$  and  $\beta$  for the tachyon inflation in the presence of a minimal length, leading to observationally viable values of  $r - n_T$ , in confrontation with Planck2018 TT, TE, and EE+lowE+lensing+BK14+BAO+LIGO and Virgo2016 data at 68% CL (dark blue) and 95% CL (light blue).

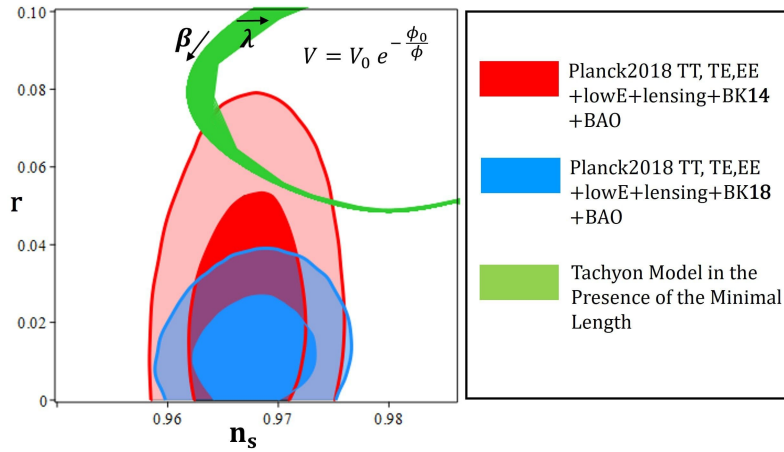


Figure 9: Tensor-to-scalar ratio versus the scalar spectral index for the tachyon inflation with inverse exponential potential in the presence of a minimal measurable length, in the background of Planck2018 TT, TE, EE +lowE+lensing+BK14+BAO and Planck2018 TT, TE, EE +lowE+lensing+BK18+BAO data. The arrows show the direction where the parameters increase.

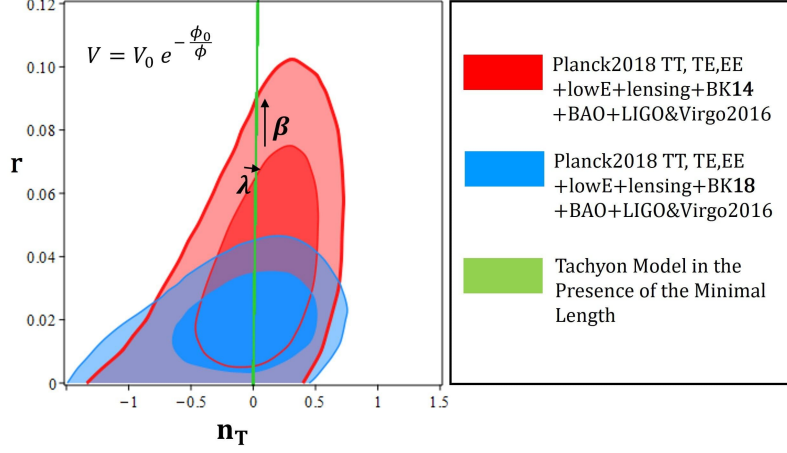


Figure 10: Tensor-to-scalar ratio versus the tensor spectral index for the tachyon inflation with inverse exponential potential in the presence of a minimal measurable length, in the background of Planck2018 TT, TE, EE +lowE+lensing+BK14+BAO+LIGO and Virgo2016 and Planck2018 TT, TE, EE +lowE+lensing+BK18+BAO+LIGO and Virgo2016 data. The arrows show the direction where the parameters increase.

Table 10: Ranges of the parameter  $\beta$  in which the tensor-to-scalar ratio, scalar spectral index and tensor spectral index of the tachyon model with  $\exp\left(-\frac{\phi}{\phi_0}\right)$  potential in the presence of a minimal length are consistent with different joint data sets.

	Planck2018 TT,TE,EE+lowE+lensing+BK18+BAO	Planck2018 TT,TE,EE+lowE+lensing+BK18+BAO	Planck2018 TT,TE,EE+lowE+lensing+BK18+BAO+LIGO&Virgo2016	Planck2018 TT,TE,EE+lowE+lensing+BK18+BAO+LIGO&Virgo2016
$\lambda$	68% CL	95% CL	68% CL	95% CL
0.1	Not Consistent	Not Consistent	$-7.42 \times 10^{-3} < \beta < -2.97 \times 10^{-8}$	$-9.07 \times 10^{-3} < \beta < 0$
0.4	Not Consistent	Not Consistent	$-2.97 \times 10^{-2} < \beta < -1.22 \times 10^{-7}$	$-3.63 \times 10^{-2} < \beta < 0$
0.7	Not Consistent	Not Consistent	$-5.21 \times 10^{-2} < \beta < -1.57 \times 10^{-7}$	$-6.36 \times 10^{-2} < \beta < 0$
1	Not Consistent	Not Consistent	$-7.46 \times 10^{-2} < \beta < -1.32 \times 10^{-7}$	$-9.12 \times 10^{-2} < \beta < 0$

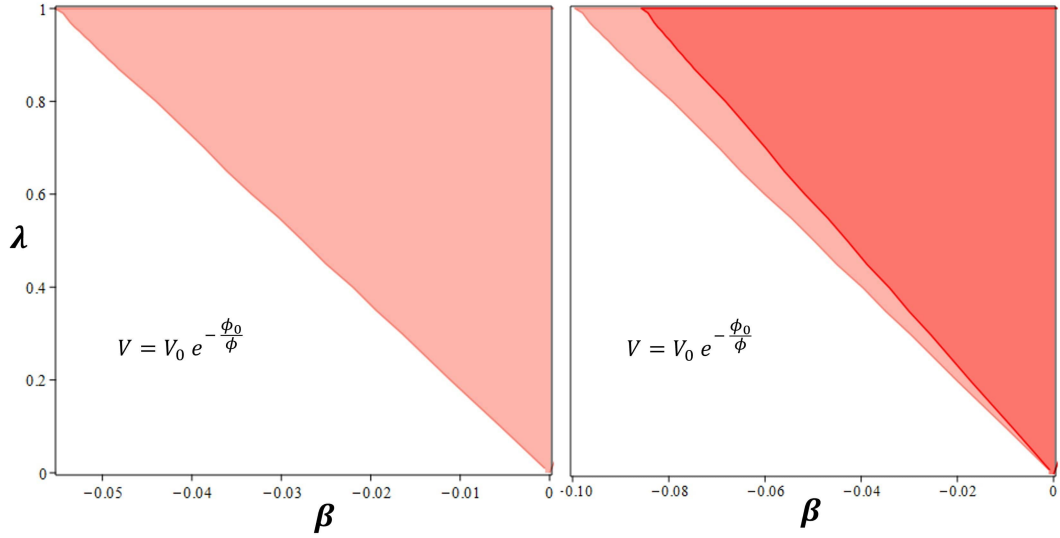


Figure 11: Left panels: ranges of the parameters  $\lambda$  and  $\beta$  for the tachyon inflation in the presence of a minimal length, leading to observationally viable values of  $r - n_s$ , in confrontation with Planck2018 TT, TE, and EE+lowE+lensing+BAO+BK14 data at 95% CL (light red). Right panels: ranges of the parameters  $\lambda$  and  $\beta$  for the tachyon inflation in the presence of the minimal length, leading to observationally viable values of  $r - n_T$ , in confrontation with Planck2018 TT, TE, and EE+lowE+lensing+BK14+BAO+LIGO and Virgo2016 data at 68% CL (dark red) and 95% CL (light red).

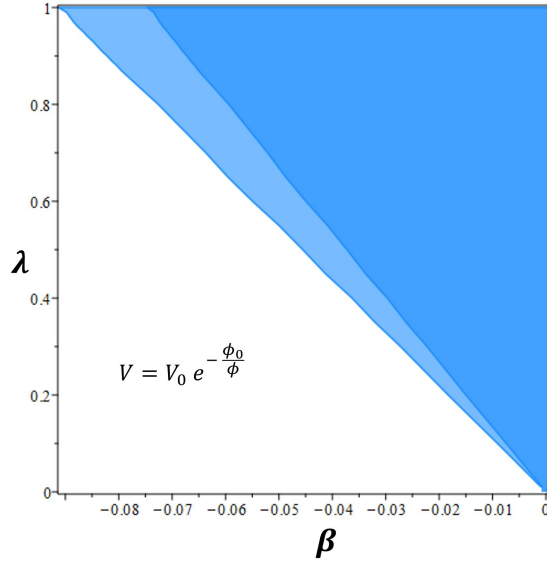


Figure 12: Ranges of the parameters  $\lambda$  and  $\beta$  for the tachyon inflation in the presence of a minimal length, leading to observationally viable values of  $r - n_T$ , in confrontation with Planck2018 TT, TE, and EE+lowE+lensing+BK14+BAO+LIGO and Virgo2016 data at 68% CL (dark blue) and 95% CL (light blue).

viable. In fact, the authors of Ref. [56] have obtained the observationally viable domain in parameter space of  $\lambda - m^2$  and also  $\lambda - v$ . However, for values of  $\lambda$  and  $v$  that we have fixed here, the tachyon model with  $0 < \lambda \leq 1$  is not consistent with Planck2018 data. This fact has also been confirmed with our analysis. In our all numerical analysis and for all  $0 < \lambda \leq 1$  we obtain  $\beta \neq 0$  to get observational viability.

According to our numerical analysis, the tachyon model in the presence of the minimal length is consistent with several data sets as follows:

- The model with  $\phi^2$  potential is consistent with Planck2018 TT, TE, EE +lowE+lensing+BK14 +BAO data at 95% CL, if  $-3.35 \times 10^{-7} \leq \beta \leq -1.37 \times 10^{-8}$  and  $-2.00 \times 10^{-4} \leq \beta \leq -2.00 \times 10^{-5}$ , depending on the value of  $\lambda$ .
- This model is consistent with the same data at 68% CL if  $-2.90 \times 10^{-7} \leq \beta \leq -1.60 \times 10^{-8}$ .
- The model with  $\phi^4$  potential is consistent with Planck2018 TT, TE, EE +lowE+lensing+BK14 +BAO data at 95% CL, if  $-1.08 \times 10^4 \leq \beta \leq -4.56 \times 10^2$ .
- With  $\phi^4$  potential, there is consistency with the data at 68% CL, if  $-9.44 \times 10^3 \leq \beta \leq -5.53 \times 10^2$ .
- With  $\phi^2$  potential, if we consider Planck2018 TT, TE, EE +lowE+lensing+BK18 +BAO data, the constraint on the parameter  $\beta$  is  $-2.49 \times 10^{-7} \leq \beta \leq -1.37 \times 10^{-8}$  at 95% CL.
- With the same data, the constraint on  $\beta$  is  $-2.73 \times 10^{-7} \leq \beta \leq -1.66 \times 10^{-8}$  at 68% CL, depending on the value of  $\lambda$ .
- With  $\phi^4$  potential, if we consider Planck2018 TT, TE, EE +lowE+lensing+BK18 +BAO data, the constraint on the parameter  $\beta$  is  $-1.04 \times 10^4 \leq \beta \leq -4.51 \times 10^2$  at 95% CL.
- With the same data, the constraint on  $\beta$  is  $-8.95 \times 10^3 \leq \beta \leq -4.51 \times 10^2$  at 68% CL, depending on the value of  $\lambda$ .
- With  $\phi^{-2}$  potential and based on Planck2018 TT, TE, EE +lowE+lensing+BK14 +BAO data, the model is observationally viable if  $-45.5 \leq \beta \leq -1.03 \times 10^{-1}$  at 95% CL.
- With the same data and same potential, we find observational viability if  $-4.56 \leq \beta \leq -1.04 \times 10^{-1}$  at 68% CL.
- Considering  $\phi^{-4}$  potential and Planck2018 TT, TE, EE +lowE+lensing+BK14 +BAO data, our setup is consistent with observation if  $-2.45 \times 10^{-5} \leq \beta \leq -8.10 \times 10^{-8}$  at 95% CL.
- With the same potential and data, there is consistency at 68% CL if  $-1.93 \times 10^{-5} \leq \beta \leq -1.25 \times 10^{-7}$ .
- The tachyon model with inverse exponential potential is consistence with Planck2018 TT, TE, EE +lowE+lensing+BK14 +BAO data at 95% CL if  $-5.53 \times 10^{-2} \leq \beta \leq -2.20 \times 10^{-8}$  at 95% CL.

- If we consider Planck2018 TT, TE, EE +lowE+lensing+BK18 +BAO data, our model with  $\phi^{-2}$ ,  $\phi^{-4}$  and inverse exponential potentials is not observationally viable.

In the above list, we have only considered Planck2018 TT, TE, EE +lowE+lensing+BK14(18) +BAO data. This is because the mentioned constraints overlap with Planck2018 TT, TE, and EE+lowE+lensing+BK14(18)+BAO+LIGO and Virgo2016 data. Therefore, the list actually covers the constraints from both data. In conclusion, considering the effects of the minimal length in the tachyon inflation makes the model observationally viable, at least in some subspaces of the model parameters space. Based on our analysis and the obtained constraints, it seems that when we consider  $\phi^4$  potential, the modification to the uncertainty relation needed to make the model viable is almost big and of the order of  $10^2 - 10^3$ . However, with  $\phi^2$ ,  $\phi^{-2}$  and  $\phi^{-4}$  potentials, this modification is very small and of the order of  $10^{-8} - 10^{-7}$ . Another case is corresponding to the inverse exponential potential leading to the modification of the order of  $10^{-8} - 10^{-3}$  which is small. Therefore, it seems that the order of the modification to the uncertainty is model-dependent.

## 6 Conclusion

In this paper, we have studied tachyon inflation by considering the quantum gravitational effects, encoded in the existence of a minimal measurable length, that seem to be important in the early universe. To this end, we have started by reviewing the construction of the modified Friedmann equations in the context of the first law of thermodynamics. In this reconstruction, the modified Friedmann equations are obtained by considering the work density in terms of the trace of the energy-momentum tensor and also assuming a general expression for the entropy. On the other hand, when we deal with the early universe, the quantum gravitational effects are naturally important. In this regard, and by considering a minimal measurable length in the theory, we have presented the modified Friedmann equations of the tachyon model. The reason for dealing with tachyon inflation is the string nature of tachyon which obviously has something to do with quantum gravitational effects. Especially, the minimal length is of the order of string length. The presence of the minimal length shows itself by a deviation parameter  $\beta$ , in the Friedmann equations. When the Friedmann equations are modified, as a result, the slow-roll parameters of inflation are modified too. We have obtained the modified slow-roll parameters in the tachyon model where the effect of the presence of minimal length appears explicitly. Since the existence of a minimal length modifies the momentum operator, and therefore the wave number, the perturbation parameters get modified. We have obtained the scalar and tensor spectral indices and also the tensor-to-scalar ratio for the tachyon model in the presence of the minimal length. After that, we have performed some numerical analysis on these parameters. In this regard, we have considered several types of potential as  $\phi^2$  and  $\phi^4$ ,  $\phi^{-2}$ ,  $\phi^{-4}$ , and inverse exponential, and performed our analysis based on these potentials. We have compared  $r - n_s$  behavior of our model with both Planck2018 TT, TE, EE +lowE+lensing+BK14 +BAO and Planck2018 TT, TE, EE +lowE+lensing+BK18 +BAO data. We have also analyzed  $r - n_T$  behavior in confrontation with Planck2018 TT, TE, EE +lowE+lensing+BK14+BAO +LIGO and Virgo2016 and Planck2018 TT, TE, EE +lowE+lensing+BK18+BAO +LIGO and Virgo2016 data. In this way, we have obtained the observationally viable ranges of the model's parameters  $\lambda$  and  $\beta$  in comparison to several data sets. Based on our analysis, it is seen that by considering the presence of the minimal length in

the tachyon inflation makes the model observationally viable. This is an important result since tachyon inflation for the mentioned potentials was ruled out in the absence of minimal length.

### ACKNOWLEDGMENTS

We thank the referees for the very insightful comments that have improved the quality of the paper considerably.

## References

- [1] D. Amati, M. Ciafaloni & G. Veneziano, *Phys. Lett. B* **216**, 41-47 (1989).
- [2] R. Casadio, O. Micu & P. Nicolini, *Fundam. Theor. Phys.* **178**, 293-322 (2015).
- [3] D. J. Gross & P. F. Mende, *Nucl. Phys. B* **303**, 407-454 (1988).
- [4] T. Yoneya, *Mod. Phys. Lett. A* **4**, 1587 (1989).
- [5] K. Konishi, G. Paffuti & P. Provero, *Phys. Lett. B* **234**, 276-284 (1990).
- [6] C. Rovelli & L. Smolin, *Nucl. Phys. B* **442**, 593-622 (1995).
- [7] A. Ashtekar & J. Lewandowski, *Class. Quant. Grav.* **14**, A55-A82 (1997).
- [8] A. Ashtekar & J. Lewandowski, *Adv. Theor. Math. Phys.* **1**, 388-429 (1998).
- [9] L. Modesto, *Class. Quant. Grav.* **26**, 242002 (2009).
- [10] O. Lauscher & M. Reuter, *JHEP* **10**, 050 (2005).
- [11] M. Reuter & J. M. Schwindt, *JHEP* **01**, 070 (2006).
- [12] R. Percacci & G. P. Vacca, *Class. Quant. Grav.* **27**, 245026 (2010).
- [13] A. Eichhorn, *Front. Astron. Space Sci.* **5**, 47 (2019).
- [14] N. Seiberg & E. Witten, *JHEP* **09**, 032 (1999).
- [15] A. Connes, *J. Math. Phys.* **41**, 3832-3866 (2000).
- [16] A. Ashtekar, S. Fairhurst & J. L. Willis, *Class. Quant. Grav.* **20**, 1031-1062 (2003).
- [17] S. Hossenfelder, *Living Rev. Rel.* **16**, 2 (2013).
- [18] L. Kofman & A. Linde, *JHEP* **0207**, 004 (2002).
- [19] A. Kempf, G. Mangano & R. B. Mann, *Phys. Rev. D* **52**, 1108-1118 (1995).
- [20] K. Nozari and A. Etemadi, *Phys. Rev. D* **85**, 104029 (2012).
- [21] G. Amelino-Camelia, *Int. J. Mod. Phys. D* **11**, 35-60 (2002).
- [22] J. L. Cortes and J. Gamboa, *Phys. Rev. D* **71**, 065015 (2005).

- [23] T. Jacobson, Phys. Rev. Lett. **75**, 1260 (1995).
- [24] E. Verlinde, [arXiv:hep-th/0008140] (2000).
- [25] R. G. Cai & Y. S. Myung, Phys. Rev. D **67**, 124021 (2003).
- [26] S. Nojiri, S. D. Odintsov & S. Ogushi, Int. J. Mod. Phys. A **16**, 5085 (2001).
- [27] S. Nojiri, S. D. Odintsov & S. Ogushi, Int. J. Mod. Phys. A **17**, 4809 (2002).
- [28] M. Cvetič, S. Nojiri & S.D. Odintsov, Nucl. Phys. B **628**, 295 (2002).
- [29] R. G. Cai & S. P. Kim, JHEP **0502**, 050 (2005).
- [30] A. J. M. Medved & E. C. Vagenas, Phys. Rev. D **70**, 124021 (2004).
- [31] R. J. Adler, P. Chen & D. I. Santiago, Gen. Rel. Grav. **33**, 2101 (2001).
- [32] M. Cavaglia, S. Das & R. Maartens, Class. Quant. Grav. **20**, L205 (2003).
- [33] M. Cavaglia & S. Das, Class. Quant. Grav. **21**, 4511 (2004).
- [34] B. Majumder, Phys. Lett. B **703**, 402 (2011).
- [35] A. F. Ali, JHEP **1209**, 067 (2012).
- [36] A. F. Ali, H. Nafie & M. Shalaby, Europhys. Lett. **100**, 20004 (2012).
- [37] G. Amelino-Camelia, M. Arzano & A. Procaccini, Phys. Rev. D **70**, 107501 (2004).
- [38] A. Awad & A. Farag Ali, JHEP **1406**, 093 (2014).
- [39] A. Guth, Phys. Rev. D **23**, 347 (1981).
- [40] A. D. Linde, Phys. Lett. B **108**, 389 (1982).
- [41] A. Albrecht & P. Steinhard, Phys. Rev. D **48**, 1220 (1982).
- [42] A. D. Linde, *Particle Physics and Inflationary Cosmology* (Harwood Academic Publishers, Chur, Switzerland) (1990).
- [43] A. Liddle & D. Lyth, *Cosmological Inflation and Large-Scale Structure*, (Cambridge University Press) (2000).
- [44] J. E. Lidsey, A. R. Liddle, E. W. Kolb, E. J. Copeland, T. Barreiro & M. Abney, Rev. Mod. Phys. **69**, 373 (1997).
- [45] A. Riotto, [arXiv:hep-ph/0210162] (2002).
- [46] D. H. Lyth & A. R. Liddle, *The Primordial Density Perturbation* (Cambridge University Press) (2009).
- [47] J. M. Maldacena, JHEP **0305**, 013 (2003).

- [48] A. Sen, JHEP **10**, 008 (1999).
- [49] A. Sen, JHEP **07**, 065 (2002).
- [50] A. Sen, Modern Physics Letters A **17**, 1797 (2002).
- [51] G. W. Gibbons, Phys. Lett. B **537**, 1 (2002).
- [52] S. Nojiri & S. D. Odintsov, Phys. Lett. B **571**, 1 (2003).
- [53] Z. Bouabdallaoui, A. Errahmani, M. Bouhmadi-López & T. Ouali, Phys. Rev. D **94**, 123508 (2016).
- [54] K. Rezazadeh, K. Karami & S. Hashemi, Phys. Rev. D **95**, 103506 (2017).
- [55] M. Majumdar & A.-C. Davis, Phys. Rev. D **69**, 103504 (2004).
- [56] S. Li & A. R. Liddle, JCAP **03**, 044 (2014).
- [57] P. A. R. Ade, et al., A & A **571**, A22 (2014).
- [58] P. A. R. Ade, et al., A & A **594**, A20 (2016).
- [59] M. J. Duff, NuPhB **125**, 334 (1977).
- [60] N. Aghanim, Y. Akrami, M. Ashdown, et al., A & A **641**, A6 (2020).
- [61] Y. Akrami, F. Arroja, M. Ashdown, et al., A & A **641**, A10 (2020).
- [62] P.A.R. Ade, Z. Ahmed, M. Amiri, D. Barkats, R. B. Thakur, et al. Phys. Rev. Lett. **127**, 151301 (2021).
- [63] D. Paoletti, F. Finelli, J. Valiviita & M. Hazumi, Phys. Rev. D **106**, 083528 (2022).
- [64] S. Chakraborty, R. Biswas & N. Mazumder, Nuovo Cim. B **125**, 1209 (2011).
- [65] S. Chakraborty, N. Mazumder & R. Biswas, Gen. Rel. Grav. **43**, 1827 (2011).
- [66] S. A. Hayward Class. Quant. Grav. **15**, 3147 (1998).
- [67] D. Bak, S.-J. Rey, Class. Quant. Grav. **17**, 83 (2000).
- [68] D. Christodoulou, Phys. Lett. **25**, 1596 (1970).
- [69] G. Amelino-Camelia, M. Arzano & A. Procaccini, Phys. Rev. D **70**, 107501 (2004).
- [70] C. Adami, [arXiv:quant-ph/0405005] (2004).
- [71] D. Kutasov, M. Marino & G. Moore, JHEP **0010**, 045 (2000).
- [72] N. Rashidi, M. Roushan & K. Nozari, EPL **142**, 39001 (2023).
- [73] A. Mantziris, T. Markkanen & A. Rajantie, Journal of Cosmology and Astroparticle Physics **03**, 077 (2021).